International Journal of Nanoelectronics and Materials
IJNeaM
ISSN 1985-5761 | E-ISSN 2232-1535

Facile solvothermal synthesis of MIL-53 (Al) using waste consumer PET: structural considerations

Azieyanti Nurain Azmin[a]*, and Halina Misran[a]

[a]*Nanoarchitectonic Laboratory, Department of Mechanical Engineering, Universiti Tenaga Nasional, 43000, Kajang, Selangor, Malaysia*
** Azieyanti Nurain Azmin. Tel.: +06-0389212554; e-mail: Azieyanti@uniten.edu.my*

Received 13 July 2023, Revised 20 January 2024, Accepted 29 January 2024

ABSTRACT

A facile solvothermal method was applied to synthesize MIL-53 (Al) at room temperature with an organic linker from waste consumer PET. MIL-53 (Al) was built from $Al(NO_3)_3.9H_2O$ connected by 1,4-benzenedicarboxylate (BDC) linkers. The waste plastic bottle was depolymerized to produce monomer BDC. The structural considerations of MIL-53 (Al) were done by using three different linkers, which are a pure linker, a BDC-PET linker, and a BDC-comm-PET linker. The investigation was obtained at two different aging durations of 24 hours and 48 hours. The X-ray diffraction peaks indicated the crystallization formed at diffraction planes of (110), (011), and (211), and the 48-hour samples observed higher crystallinity. Thermal analysis of samples exhibited weight loss at three stages attributed to the removal of solvent and molecules, trapping BDC, and the departure of BDC to the framework, respectively. Raman shift was obtained to show the MIL-53 (Al) structure while the FTIR spectra exhibited the absorption peaks and stretching vibrations of each group. The primary crystallite size was calculated from the Scherrer equation, and the range was between ca. 10 nm and 32 nm. Furthermore, the value observed using a William-Hall (WH) plot showed the crystallite size was almost similar in the range of ca. 8 nm to 21 nm. The FESEM morphology observed the rod-like structure of MIL-53 (Al), and the 48-hour samples observed the larger particle.

Keywords: *MIL-53 (Al), Solvothermal, Metal-organic framework, Waste plastic*

1. INTRODUCTION

Two decades ago, researchers discovered metal-organic frameworks (MOFs) as nanomaterials that have earned interest among attractive classes because of their high porosity solid crystalline structure. Their composition differs from other porous materials. MOFs are constructed from organic linkers and metal ions, while other porous materials such as zeolite are composed of inorganic materials. Other than that, the covalent organic framework is composed of organic compounds. MOFs offer various advantages, such as having a high surface area, the ability to tune the pore size, and having functional pores. The 'functional pores' of MOFs refer to the specific pores within the MOF structure that have been modified and designed for functions such as gas adsorption, catalysis, sensing, and ion exchange. The researchers can customize the function pores to suit their intended applications. Thus, these characteristics have resulted in producing more stable MOFs with higher valence numbers of metals such as zirconium, aluminum, vanadium, and iron. Further, their applications are resulting in various areas such as gas and energy storage, healthcare, and environmental remediation [1-2].

A subclass of MOF known as MIL (Material Institute Lavoisier) was first synthesized in 2002 and has exhibited thermal and water stability. Among many MOF products, MIL has high efficiency in the removal of pollutants from aqueous mediums. MIL-n, also known as the MIL family, has been synthesized from trivalent cations and linkers from carboxylic acid. Trivalent cations applied in MIL, such as Fe^{3+}, Al^{3+}, Cr^{3+}, Ga^{3+}, V^{3+}, and In^{3+}, are different with a diamond-shaped network. The diamond shape is the crystal structure or topology of the MIL family or other MOFs within the MIL family. Metal ions and linkers are arranged in repeating patterns that form a network. Thus, the network of diamond shapes describes the appearance of this network in two dimensions. Among all types of the MIL family, MIL-53 is known as the most promising MOF for chemical adsorption [3-4]. MIL-53 is built with $MO_4(OH)_2$ connected by groups of terephthalates to form a 3D building. $MO_4(OH)_2$ is known as the shared corner of octahedral chains (M=Cr, Al, Fe, In, Sc, Ga) [5].

Recently, MIL-53 (Al) has presented unique features with stability and flexibility, structure, selectivity, and recyclability. It also has a high surface area and is moisture-resistant, which makes it a promising MOF in the process of adsorption. MIL-53 (Al) stands out as an excellent aluminum-based MOF with a reputation for its affordability and cost-effectiveness. Generally, MIL-53(Al) is constructed from trans octahedral $AlO_4(OH)_2$ chains. It relates to the linker from 1,4-benzenedicarboxylate (BDC) to form a framework. Its structure has large and opened internal pores, forming like a 'wine rack', due to the

presence of solvents and ligands/linkers. Furthermore, MIL-53 (Al) demonstrates extensive interest in the applications of separation, catalysis, and adsorption capacity in the removal of dyes, heavy metals, and pharmaceuticals [4-6].

Furthermore, this work is being developed to address the global issue of increasing waste of consumer plastic (WCP). The gradual rise of WCP over time poses significant threats to our economy, as well as alarming ecological pollution. WCP from PET (polyethylene terephthalate) has received considerable attention because of its annual worldly consumption at ca. 34 billion tonnes until 2050. As reported, due to poor biodegradability, the huge consumption of PET bottles makes them one of the most abundant wastes on earth. Therefore, it is necessary to approach efficient plastic waste recycling. One of the proposed initiatives is utilizing PET as the primary material during the synthesis of MOFs. The monomers of PET known as (benzene-1,4-dicarboxylic acid, BDC, or terephthalate acid), can be upcycled to produce MOFs as organic linkers [7]. This effort can tackle the green and eco synthesis of functional materials from these waste materials and get public attention as a point of environmental protection and energy saving [8-9]. The BDC linker was derived through depolymerization. The conversion of PET into a monomer can be achieved via methods like hydrolysis, glycolysis, or ethanolysis [3,10-12]. By using a similar strategy, it is very economical as it reduces production costs, and is valuable for the environment [13]. Further, being innovative in waste PET usage during the synthesis and production will also allow for the creation and production of a high–value end-use product [14-16] and luckily, BDC is a perfect organic linker in MOF structures [17]. Additionally, previous research also reported the waste PET bottle as the precursor for the synthesis of MIL-*n* [18-20].

Therefore, in this experiment, MIL-53 (Al) was produced by using simple solvothermal synthesis. This process is more accessible and efficient, involving a solvent, elevated temperature, and pressure. Solvothermal methods are considered cost-effective and environmentally friendly for synthesizing inorganic materials. They occur at lower temperatures, are easy to control, and can produce samples with regular and uniform morphology with good dispersion [21]. Three different linkers were used in this experiment: pure linkers from terephthalic acid, BDC-PET linkers from WCP drinking bottles, and BDC-comm-PET linkers from Sigma Aldrich.

2. MATERIALS AND METHODS

2.1. Raw Materials

In this research, the raw materials used are as follows: Aluminium nitrate nanohydrate ($Al(NO_3)_3.9H_2O$, Thermo Scientific), N,N-dimethylformamide (DMF, Merck, 99.8%), terephthalic acid ($C_8H_6O_4$, 1, 4-benzene dicarboxylic acid, H_2BDC, Merck, 98%), flakes cut from waste PET drinking bottles, PET granular/pellet form (Sigma Aldrich), ethylene glycol (Sigma Aldrich, 99.8%), ethanol, acetone, and deionized (DI) water. All raw materials were used without further purification.

2.2. Depolymerization Process

WCP from plastic PET drinking bottles went through a depolymerization process known as glycolysis [22]. PET was cut into flakes in size 5mm x 3mm from plastic drinking bottles and mixed with a 50ml solution of ethylene glycol and DI water, then placed in an autoclave with Teflon-lined stainless steel. After five hours of reaction at 210°C, it was centrifuged with ethanol and continued to dry in a vacuum oven at 100°C overnight. This linker was labeled as a BDC-PET linker. The method was repeated by commercial PET granules from Sigma Aldrich. This linker was labeled as a BDC-comm-PET linker.

2.3. MIL-53 (Al) Solvothermal Synthesis

Solvothermal synthesis: Terephthalic acid was used as a pure linker and was sonicated with DMF and DI water, followed by the addition of $Al(NO_3)_3.9H_2O$. The sonication continued for 15 minutes. Then, the solution was placed in an autoclave lined with Teflon-lined stainless steel. The reaction of the mixture in a drying oven took 24 hours at 150 °C. After the reaction, they were cooled at room temperature, centrifuged with DMF and acetone, and then continued the activation process by drying in a vacuum oven at 70 °C for 24 hours. The process was repeated for linker BDC-PET and linker BDC-comm-PET and repeated for 48 hours of aging duration. Figure 1 shows the schematic diagram of the depolymerization and solvothermal synthesis processes of MIL-53 (Al). The synthesis parameter is shown in Table 1 below.

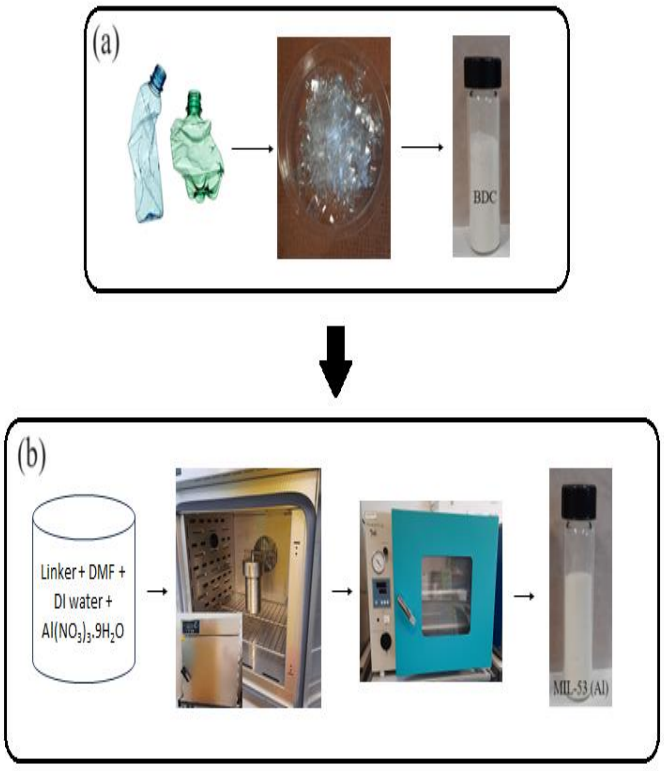

Figure 1 (a) Depolymerization of PET, and (b) solvothermal synthesis of MIL-53 (Al)

Table 1 Synthesis parameter of MIL-53 (Al) (1) - MIL-53 (Al) (6)

Sample	Linker	DMF, DI water	Aging duration	Drying condition
MIL-53 (Al) (1)	Terephthalic acid	√	150°C, 24 hours	70°C, 24 hours
MIL-53 (Al) (2)	Terephthalic acid	√	150°C, 48 hours	70°C, 24 hours
MIL-53 (Al) (3)	BDC-PET	√	150°C, 24 hours	70°C, 24 hours
MIL-53 (Al) (4)	BDC-PET	√	150°C, 48 hours	70°C, 24 hours
MIL-53 (Al) (5)	BDC-comm-PET	√	150°C, 24 hours	70°C, 24 hours
MIL-53 (Al) (6)	BDC-comm-PET	√	150°C, 48 hours	70°C, 24 hours

2.4. Structural Characterizations

X-ray diffractograms/diffractions (XRD) were indicated by a Shimadzu XRD-6000. The X-ray operated at 30 kV voltage and 20 mA current. The diffractions were recorded with a scan speed of 3°/min in the 5°—45° 2θ range. The Scherrer equation and William and Hall (WH) plot will estimate the primary crystallite size. The uniform deformation model (UDM) from the WH plot can be calculated by [23]:

$$\beta \cos \theta = 4C_{\varepsilon} \sin \theta + k\lambda/D \quad (1)$$

where β is the FWHM value (in radians), θ is the Bragg diffraction angle (in radians), C_{ε} is the value of strain, K is a constant due to the shape factor (0.9), and λ is the wavelength of the incident X-ray used (1.5406 Å). Then, β cos θ was plotted as the *y*-axis against 4 sin θ as the *x*-axis to form a Lorentzian graph. The graph will form the intercept value, which is used to obtain the crystallite size. Relative crystallinity (RC) was calculated by taking the highest percentage of the relative intensity of the sample.

IR Prestige-21 Shimadzu was used to evaluate Fourier transform-infrared spectroscopy (FTIR) analyses. The setup wavenumbers were 500 cm^{-1}—4000 cm^{-1}. Raman spectroscopy was carried out to identify the chemical composition using RENISHAW via a Raman microscope with an excitation wavelength of 532 nm and 1% laser power. A Hitachi SU 8020 operating at an acceleration voltage of 15kV was used for field emission scanning electron microscopy (FESEM). Thermogravimetric analysis (TGA) was performed in air at 100ml/min, in the temperature range of 25°—900°, with a 10°C/min of temperature rate (Shimadzu DTG-60) [23].

3. RESULTS AND DISCUSSION

Figure 2 observed the diffraction peaks of MIL-53 (Al) (1) – MIL-53 (Al) (6). The diffraction patterns have shown the crystalline nature between 9—25°. The high peaks indicate the samples have high crystallinity. The patterns are similar and match well between all three different linkers. The peaks of the samples with an aging duration of 48 hours indicate higher crystallinity as compared to the samples with an aging duration of 24 hours. The reason is the extended aging duration can provide more time for these reactions to process, thus leading to the formation of larger crystallites as the sample structure becomes more thermodynamically stable. All the diffraction peak (2θ) values were at ca. 9°, 15°, and 18°, corresponding to (110), (011), and (211) crystal planes. Notably, the observed XRD pattern for the sample with the WPC linker matches well with the pristine sample.

Table 2 shows the crystallite size calculation by the Scherrer equation and WH plot, and the relative crystallinity (RC). Relative crystallinity represents each sample as a percentage based on the summation of major peak intensities relative to the best crystallinity [5]. To calculate the RC values, the sample with 100% crystallinity was used as the baseline. MIL-53 (Al) (2) is selected as the indicator for having the highest (110) crystal plane. The RC values for MIL-53 (Al) (1), (3), (4), (5), and (6) are 50%, 65%, 96%, 28%, and 48%, respectively. According to the Scherrer equation, the primary crystallite size ranges from ca. 10 nm to 32 nm. Figure 3 shows the Williamson-Hall (WH) plots of the samples, with the crystallite size from the WH plot estimated at around 8 nm to 21 nm. The crystallite sizes obtained from these two equations are almost similar. Furthermore, the samples with an aging duration of 24 hours showed lower crystallite sizes due to the low relative crystallinity. This might also be associated with the mismatch in the grafting of the structure compared to its natural pristine growth [24]. Among all samples, the one with a BDC-comm-PET linker exhibits the highest crystallite size for both aging durations compared to other linkers.

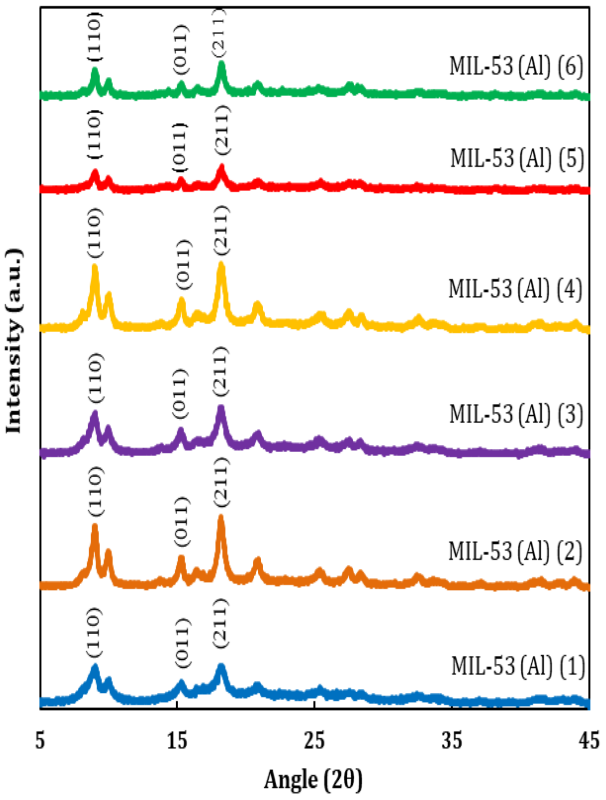

Figure 2 X-ray diffraction patterns of MIL-53 (Al) (1) – MIL-53 (Al) (6)

Table 2 Relative crystallinity (RC) and crystallite size of MIL-53 (Al) (1) - MIL-53 (Al) (6)

Sample	Relative crystallinity (RC) (%)	Crystallite size (nm) by Scherrer equation	Crystallite size (nm) by WH plot
MIL-53 (Al) (1)	50	10	8
MIL-53 (Al) (2)	100	16	16
MIL-53 (Al) (3)	65	11	12
MIL-53 (Al) (4)	96	16	14
MIL-53 (Al) (5)	28	32	18
MIL-53 (Al) (6)	48	28	21

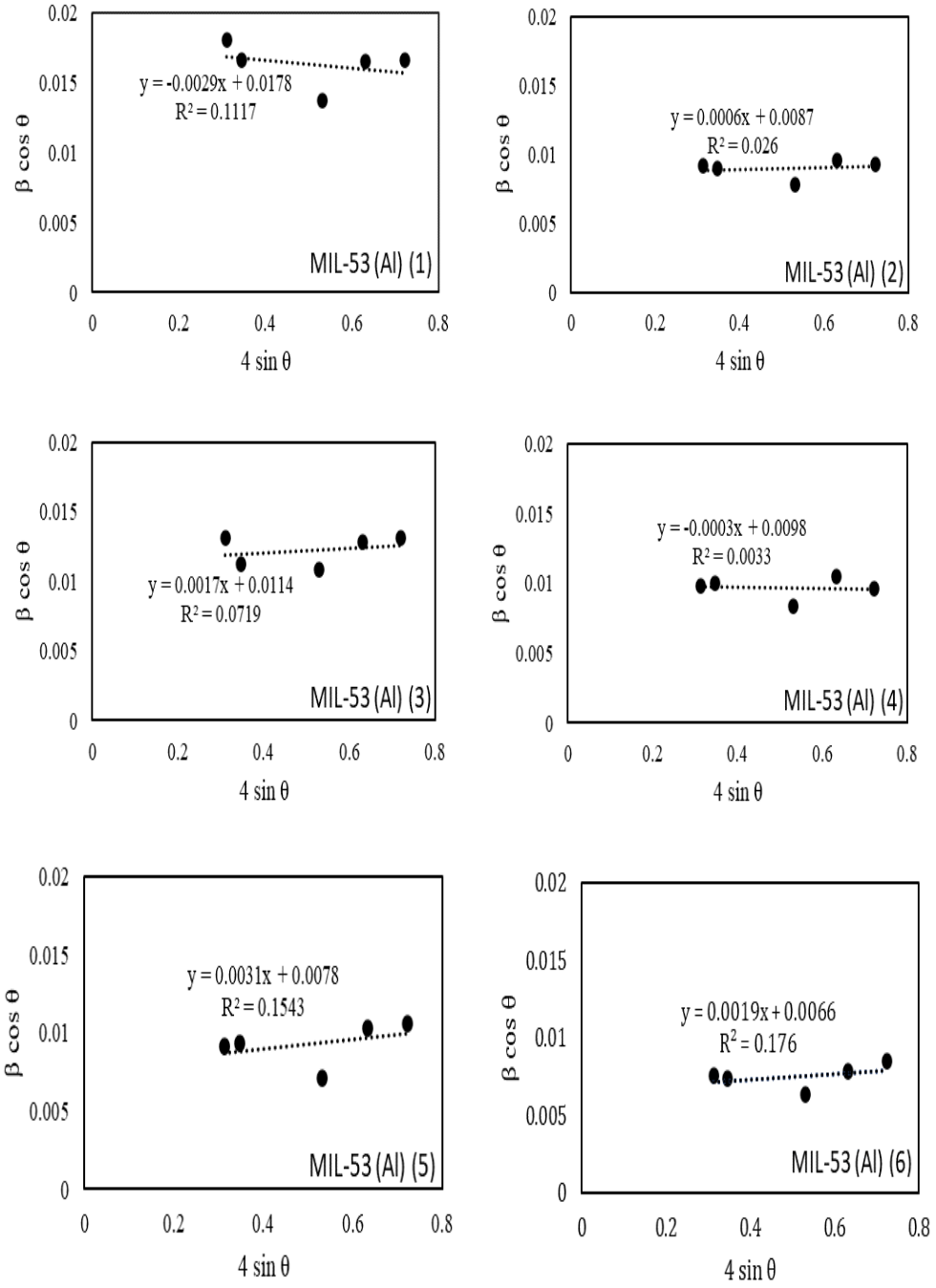

Figure 3 The Williamson-Hall (WH) plots of MIL-53 (Al) (1) – MIL-53 (Al) (6)

The FTIR spectrum was used to investigate the functional group of the sample. Figure 4 displays the MIL-53 (Al) spectrum for all samples. From the graph, the C=O stretching vibration was obtained at the peak of 1375 cm^{-1}. This is due to the stretching vibration peak of the carboxyl group in the uncoordinated ligand of terephthalic acid which is trapped in the framework. The peak at 1431 cm^{-1} corresponded to the C=C benzene ring from terephthalic acid/BDC. The asymmetric stretching vibration of the COO functional group corresponds to the two peaks at 1045 cm^{-1} and 1055 cm^{-1} while at 3305 cm^{-1} wide peak is related to OH stretching vibration. The aromatic C-H curving vibration in-plane bending was identified at the peak of 877 cm^{-1} [2]. Furthermore, as observed in Figure 5, MIL-53 (Al) in this work exhibited Raman shift at 872 cm^{-1}, 1149 cm^{-1}, 1452 cm^{-1}, 1474 cm^{-1}, and 1616 cm^{-1} which corresponds to MIL-53 (Al) (3) structure.

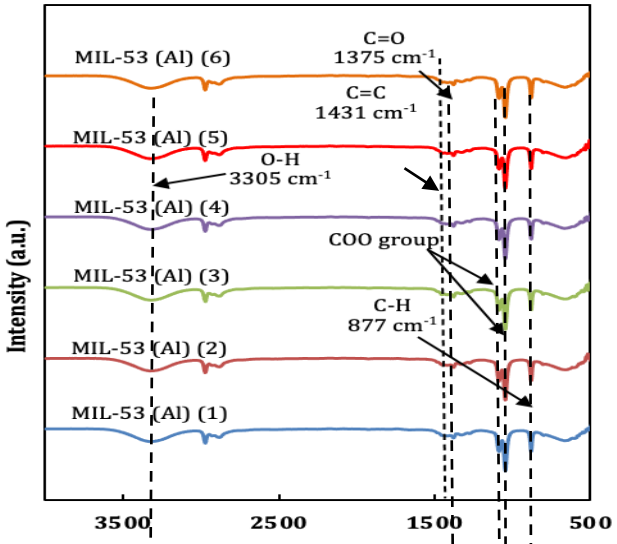

Figure 4 FTIR spectra of MIL-53 (Al) (1) - MIL-53 (Al) (6)

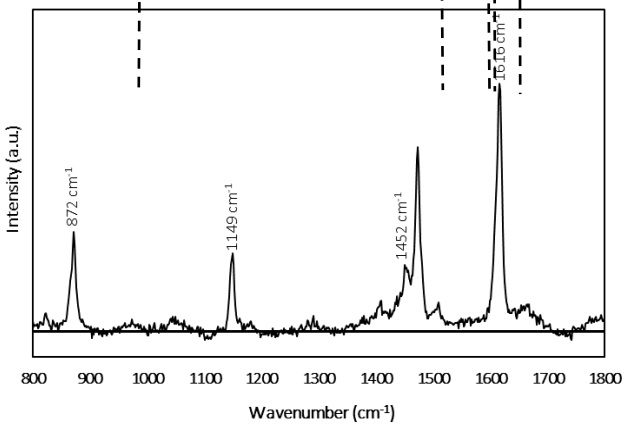

Figure 5 Representative RAMAN spectrum of MIL-53 (Al) (3)

The morphologies of MIL-53 (Al) (1) – MIL-53 (Al) (6) were investigated by FESEM as shown in Figure 6. The images show an aggregated rod-like structure for both 24-hour and 48-hour durations. The images of the 24-hours samples showed fine particles compared to the 48-hours samples. With the increasing reaction duration, the particle size of the samples is getting larger. This is due to the favor of crystal growth. Further, the particle size of the sample with BDC-comm-PET shows the biggest size as compared to others. Figure 7 illustrates the thermal stability of MIL-53 (Al) (1) – MIL-53 (Al) (6), respectively. The samples show the initial weight loss of ca. 80°C—300°C, due to the presence of moisture which is due to the removal of solvent and small molecules [6,25]. This is called the dehydration process where the compound reversibly adsorbs and desorbs the water from the environment [26]. Then, the second weight loss is further dropped with the increased temperature due to the BDC linker trapped in the framework pores. It occurred at temperatures between ca. 300°C—420°C. The third event occurred between ca. 700°C—850°C associated with the departure of the BDC linker to form the framework, thus collapsing the structure. According to the analyses, the samples are completely decomposed at 900°C.

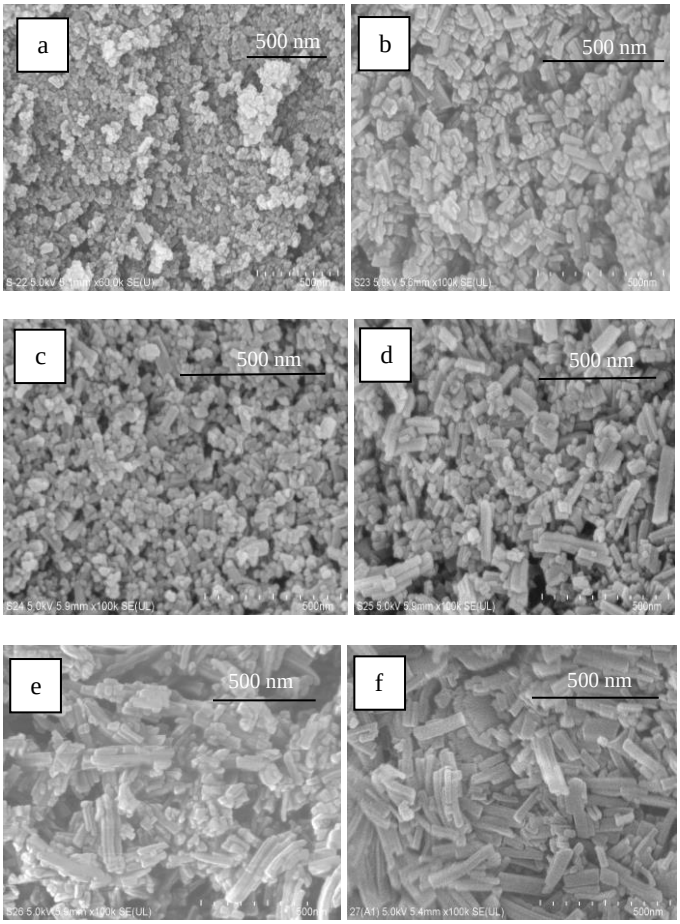

Figure 6 FESEM micrographs of (a) MIL-53 (Al) (1), (b) MIL-53 Al (2), (c) MIL-53 Al (3), (d) MIL-53 Al (4), (e) MIL-53 Al (5), and (f) MIL-53 (Al) (6)

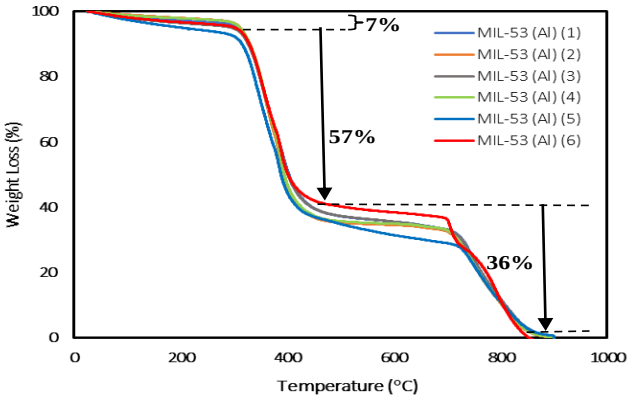

Figure 7 Thermal stability of MIL-53 (Al) (1) – MIL-53 (Al) (6)

4. CONCLUSION

This research successfully achieved the synthesis of MIL-53 (Al) with a pure linker, and the linker derived from BDC-PET, and BDC-comm-PET via a straightforward and convenient solvothermal method at room temperature. A comprehensive structure assessment was conducted on all samples, encompassing bonding analysis, phase analysis, chemical analysis, morphology, and thermal analysis. The formation of well-defined crystals was inferred from XRD peaks, which exhibited variations based on the choice of the linker, thus resulting in the percentage of relative crystallinity and crystallite size of all samples. FTIR spectroscopy revealed the functional groups in the samples and provided the chemical bond and molecular structure, the same goes for the RAMAN shift analysis, which confirmed the MIL-53 (Al) molecular structure but is more sensitive to polarizability. Both analyses provide insights into the chemical composition and MIL_53 (Al) structure. Additionally, FESEM images confirmed the rod-like morphology of the samples with the bigger particle size and the increasing aging duration. The thermal stability exhibited the percentage weight loss attributed to the solvent and molecules removal, trapping, and release of BDC to the framework. Overall, the choice of linker appears to have an impact on the resulting structure and properties of the MIL-53 (Al) metal-organic framework.

REFERENCES

[1] Tongrong W., Nicholaus, and Kang L., "Recent advances in aluminium-based metal-organic frameworks (MOF) and its membrane applications," *Journal of Membrane Science*, vol. 615, p. 118493, 2020.

[2] Zolfa Z., Niyaz M. M., Mohammad R. R., and Alireza S., "Synthesis of visible light activated metal-organic framework coated on titania nanocomposite (MIL-53(Al)@TiO2) and dye photodegradation," *Journal of Solid State Chemistry*, vol. 307, p. 122747, 2022.

[3] Ahmad A., Asma A. A., Wafa J. A., Norah A., Amal M. A.-M., Ayman G., Zeid A. A., and Ahmed-Y. B.-H.-A., "Synthesis of value-added MIL-53(Cr) from waste polyethylene terephthalate bottles for the high-performance liquid chromatographic determination of methylxanthines in tea," *Microchemical Journal*, vol. 167, p. 106294, 2021.

[4] Hamza A. I., Khairulazhar J, Nonni S. S., Zakariyya U. Z., Nor A. F. A., and Bahruddin S., "Effective adsorption of metolachlor herbicide by MIL-53(Al) metal-organic framework: Optimization, validation and molecular docking simulation studies," *Environmental Nanotechnology, Monitoring & Management*, vol. 18, p. 100663, 2022.

[5] Armin T., Ensieh Ganji Babakhani, and Jafar T., "Study of synthesis parameters of MIL-53(Al) using experimental design methodology for CO2/CH4 separation," *Adsorption Science & Technology*, vol. 36, issue 1–2, pp. 247–269, 2018.

[6] Liwei S., Meilin Y., Zhen L., and Shaokun T., "Facile microwave-assisted solvothermal synthesis of rod-like aluminum terephthalate [MIL-53(Al)] for CO2 adsorption," *Journal of Industrial and Engineering Chemistry*, vol. 112, pp. 279–286, 2022.

[7] Ademola B. R., Zainura Z. N., Azman H., Mohd K. A. H., Sani A. S., and Ali H. S., "Current developments in chemical recycling of post-consumer polyethylene terephthalate wastes for new materials production: A review," *Journal of Cleaner Production*, vol. 225, pp. 1052–1064, 2019.

[8] Yong-J. C., Xianqiang H., Yifa C., Yi-R. W., Haichao Z., Chun-X. L., Lei Z., Hongjing Z., Ruxin Y., Yu-H. K., Shun-L. L., and Ya-Q. L., "Polyoxometalate-Induced Efficient Recycling of Waste Polyester Plastics Into Metal–Organic Frameworks," *CCS Chem.*, vol. 1, pp. 561–570, 2019.

[9] Xoliswa L. D., and Jianwei R., "High value-added metal-organic frameworks from polyethylene terephthalate waste as linker source," in *PET-MOF-CLEANWATER Project*, Chapter 4, 2020.

[10] Xoliswa D., Jianwei R., Nicholas M. M., Henrietta W. L., Mkhulu K. M., and Maurice O., "Feasibility of varied polyethylene terephthalate wastes as a linker source in metal-organic framework UiO-66(Zr) synthesis," *Ind. Eng. Chem. Res.*, vol. 58, issue 36, pp. 17010–17016, 2019.

[11] Xiang-J. K. and Jian-R. L., "An Overview of Metal–Organic Frameworks for Green Chemical Engineering," *Engineering*, vol. 7, issue 8, pp. 1115-1139, 2021.

[12] George P. K. and Dimitris S. A., "Chemical Recycling of Poly(ethylene terephthalate)," *Macromolecular Materials and Engineering*, vol. 292, pp. 128-146, 2007.

[13] Jorge B., Virginia M.-R., Manuel P.-G., Almudena G.-A., Juan J. R., and Carolina B., "A Review on the Synthesis and Characterization of Metal Organic Frameworks for Photocatalytic Water Purification," *Catalysts*, vol. 9, p. 52, 2019.

[14] Meicheng W., Guiying L., Hongli L., Jiangyao C., Taicheng A., and Hiromi Y., "Metal–organic framework-based nanomaterials for adsorption and photocatalytic degradation of gaseous pollutants: recent progress and challenges," *Environmental Science: Nano*, vol. 6, pp. 1006-1025, 2019.

[15] Juan L., Ji-L. G., Guang-M. Z., Peng Z., B. S., Wei-C. C., Hong-Y. L., and Shuang-Y. H. J., "Zirconium-based metal organic frameworks loaded on polyurethane foam membrane for simultaneous removal of dyes with different charges," *Colloids and Interface Science*, vol. 527, pp. 267–279, 2018.

[16] Juan L., Hou W., Xingzhong Y., Jingjing Z., and Jia W. C., "Metal-organic framework membranes for wastewater treatment and water regeneration," *Coordination Chemistry Reviews*, vol. 404, p. 213116, 2020.

[17] Van D. D., Thi L. D., Thi M. T. H., Van T. L., and Hoai T. N., "Utilization of waste plastic PET bottles to prepare copper-1,4-benzenedicarboxylate metal-organic framework for methylene blue removal," *Separation Science and Technology*, vol. 55, pp. 444–455, 2019.

[18] Bahman F., Nasser D., Soheyla K., and Muhammad S. L., "Application of MIL-53(Al) prepared from waste materials for solid-phase microextraction of

propranolol followed by corona discharge-ion mobility spectrometry (CD-IMS)," *Journal of Pharmaceutical and Biomedical Analysis*, vol. 189, p. 113418, 2020.

[19] Sheng-H. L., Duraisamy S. R., Chia-W. C., Yu-H. K., Jiun-J. C., and Chia-H. L., "Waste Polyethylene Terephthalate (PET) Material as Sustainable Precursor for the Synthesis of Nanoporous MOFs, MIL-47, MIL-53(Cr, Al, Ga) and MIL-101(Cr)," *Dalton Transactions*, vol. 45, pp. 9565-9573, 2016.

[20] Willem P. R. D., Ivo S., Dries J., Rob A., and Dirk E. D. V., "Waste PET (bottles) as Resource or Substrate for MOF Synthesis," *Journal of Materials Chemistry A*, vol. 4, pp. 9519-9525, 2016.

[21] Fayza Y., Nasruddin, Agustino Z., and Rizky R., "Metal-organic framework based chromium terephthalate (MIL-101 Cr) growth for carbon dioxide capture: a review," *Journal of Advanced Research in Fluid Mechanics and Thermal Sciences*, vol. 57, issue 20, pp. 158-174, 2019.

[22] Volanti M., Cespi D., Passarini F., Neri E., Cavani F., Mizsey P., and Fozer D., "Terephthalic acid from renewable sources: Early-stage sustainability analysis of a bio-PET precursor," *Green Chemistry*, vol. 21, issue 4, pp. 885-896, 2019.

[23] Shaiful Bahari A. M., Zulkifli N. H., Azmin A. N., Alias N., Rosli S. A., Sazalli N. A. H., Lockman Z., Amin N., and Misran H., "Facile Synthesis of Chloride-less Zirconium-based Metal-Organic Framework (MOF) as Chromium (VI) Removal via Photoreduction," *Malaysian Journal of Microscopy*, vol. 17, issue 2, pp. 220-238, 2021.

[24] Thilina R. K., Chalita R., Pakorn O., Chariya K., and Paiboon S., "A smart magnetically separable MIL-53(Al) MOF-coated nano-adsorbent for antibiotic pollutant removal with rapid and non-contact inductive heat regeneration," *Chemical Engineering Journal Advances*, vol. 8, issue 7, p. 100160, 2021.

[25] Debashis P., Soumyadip P., Mahendra K. A., and Sanjay K. S., "Lab Cooked MOF for CO2 Capture: A Sustainable Solution to Waste Management," *Journal of Chemical Education*, vol. 97, issue 4, pp. 1101-1108, 2020.

[26] Oana G., Angela M. K., Alexandru T., Monica D., Lucian B. -T., Mihaela D. L., and Maria M., "Facile and efficient synthesis of ordered mesoporous MIL-53(Al)-derived Ni catalysts with improved activity in CO2 methanation," *Journal of Environmental Chemical Engineering*, vol. 11, issue 2, p. 109456, 2023.